

Chapter 2

Mechanism of Mo-Dependent Nitrogenase

Zhi-Yong Yang, Karamatullah Danyal, and Lance C. Seefeldt

Abstract

Nitrogenase is the enzyme responsible for biological reduction of dinitrogen (N_2) to ammonia, a form usable for life. Playing a central role in the global biogeochemical nitrogen cycle, this enzyme has been the focus of intensive research for over 60 years. This chapter provides an overview of the features of nitrogenase as a background to the subsequent chapters of this volume that detail the many methods that have been applied in an attempt to gain a deeper understanding of this complex enzyme.

Key words: Nitrogen fixation, Fe protein, MoFe protein, mechanism, metalloenzyme, MgATP.

1. Nitrogen Fixation

Dinitrogen (N_2) is the major constituent (79%) of the Earth's atmosphere, representing the largest global pool of nitrogen (N). While nitrogen is essential to all life, the vast reservoir of dinitrogen in the atmosphere is unusable by most organisms (1, 2). This is largely a consequence of the high bond dissociation energy for the N_2 triple bond (3), making the breaking of this bond and “fixation” of the nitrogen to forms usable to living organisms energetically challenging. Dinitrogen can be fixed with considerable energy input by addition of electrons and protons to yield two ammonia (NH_3) molecules. In the industrial Haber–Bosch process for fixing dinitrogen, the reaction is carried out at high temperatures ($\sim 450^\circ\text{C}$) and pressures (>200 atm) in the presence of an iron catalyst, with the electrons and protons coming from H_2 (1, 4–6). This process is extremely energy demanding, utilizing approximately 1% of the total fossil fuel used globally (7).

The other major pathway for reduction of dinitrogen is through the action of select microorganisms (called diazotrophs) that carry out a process called biological nitrogen fixation (6, 8). The first step in the assimilation of N_2 by these organisms is the reduction of N_2 to two ammonia molecules catalyzed by a complex metalloenzyme called nitrogenase (9, 10). Nitrogenases occur across a wide range of microbes and sequencing of the nitrogenase genes (*nif* genes) reveals considerable sequence diversity among the enzymes (10–12). Despite this sequence diversity, the majority of nitrogenases share some common features. For example, most enzymes are composed of two component proteins: a large component having at least an $\alpha_2\beta_2$ subunit composition and a smaller component having a γ_2 subunit composition. All known nitrogenases contain iron–sulfur clusters in both component proteins. The site of N_2 binding and reduction is one of the iron–sulfur clusters contained in the larger component protein. This active site metal cluster can contain, in addition to Fe atoms, a heterometal atom (Mo or V) (9, 10, 13, 14). The best studied nitrogenase is the Mo-dependent enzyme, which appears to be the paradigm for nitrogenases (9, 13, 15–21). Given that most of the mechanistic information known about nitrogenases is for the Mo-based enzyme, this chapter will focus on this enzyme. Other nitrogenases, sometimes called alternative nitrogenases, are reviewed elsewhere (10, 12).

2. Mo-Dependent Nitrogenase: Overview

The two component proteins of the Mo-dependent nitrogenase are called the iron (Fe) protein (or dinitrogenase reductase) and the molybdenum–iron (MoFe) protein (or dinitrogenase) (**Fig. 2.1**). These two component proteins work together to catalyze the reduction of dinitrogen in a complex reaction with an ideal reaction stoichiometry shown as follows (22):



A breakthrough in understanding nitrogenase came from the X-ray crystal structures of the component proteins solved individually (23–42) and when bound together (43–46). The Fe protein, the only known reductant of the MoFe protein that can support substrate reduction, is a homodimer that contains two nucleotide (MgATP or MgADP) binding sites, one on each subunit, and a single $[4Fe-4S]$ cluster that bridges the two subunits (**Fig. 2.1**) (25). The MoFe protein is an $\alpha_2\beta_2$

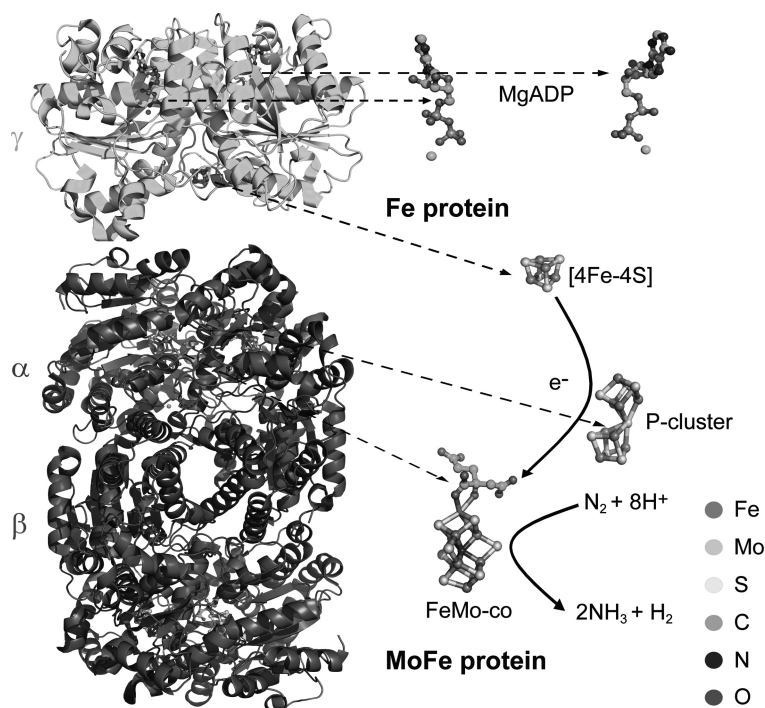


Fig. 2.1. Crystal structure of the Fe and MoFe protein components of Mo-dependent nitrogenase showing the nucleotides, metal clusters, and electron transfer pathways. (*Left*) Cartoon representation of MoFe protein (pdb code: 1M1N) with the α -subunits and the β -subunits and Fe protein (pdb code: 1FP6) with the γ -subunits. (*Right*) Structures of MgADP and the three metalloclusters of nitrogenase. The figure was generated using the computer program PyMol.

heterotetramer. Each $\alpha\beta$ dimeric unit contains two unique metalloclusters: a P-cluster ([8Fe-7S]) and an FeMo cofactor ([7Fe-9S-Mo-X-(R)-homocitrate]) (Fig. 2.1) (27, 28, 47). Each $\alpha\beta$ -unit appears to function as a catalytic unit independent of the other $\alpha\beta$ pair. During the catalytic cycle, an Fe protein binds transiently to one MoFe protein $\alpha\beta$ unit. During this encounter, one electron is transferred from the [4Fe-4S] cluster of the Fe protein to the MoFe protein. This electron transfer step is coupled to the hydrolysis of a minimum of two MgATP molecules (16, 48). Following electron transfer and ATP hydrolysis, the Fe protein disengages from the MoFe protein and a new Fe protein binds in its place to repeat the cycle. Given that only one electron is transferred per cycle, a minimum of eight encounters must occur to reduce N₂ (equation [1]).

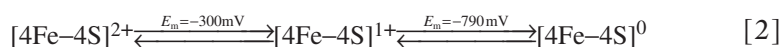
2.1. Fe Protein

The Fe protein is a homodimer (coded for by the *nifH* gene) with a molecular mass of approximately 64,000 Da (25, 49). In addition to delivering electrons to the MoFe protein, the Fe protein also is known to function in the maturation of the MoFe

protein and in the bioassembly of the active site metal cluster called FeMo cofactor (49, 50). This maturation role for the Fe protein does not appear to require electron transfer or the ATP hydrolysis function (9) and is covered in another chapter of this volume.

2.1.1. Redox Properties of the [4Fe–4S] Cluster

The Fe protein contains a single [4Fe–4S] cluster that serves as a carrier of electrons. The X-ray structure of the Fe protein revealed that this cluster is symmetrically ligated between the two Fe protein subunits, with each subunit contributing two cysteine ligands (**Fig. 2.1**). The [4Fe–4S] is known to access three redox states (9, 21):



The [4Fe–4S]^{2+/1+} redox couple is operational during substrate reduction supported by reductants such as dithionite or ferredoxin (9, 51, 52). A more reduced (0) oxidation state (termed the “all-ferrous” state) can be achieved in vitro by incubating the Fe protein with reductants with very negative potentials (e.g., Titecitrate) (53–57). It has been demonstrated that the all-ferrous state can participate in the delivery of electrons to the MoFe protein when strong reductants are used (58). However, the role of this all-ferrous state during catalysis in vivo remains unknown.

The 1+ oxidation state (Fe^{Red}) of the [4Fe–4S] cluster is the dominant state in the as-purified enzyme in the presence of the reductant dithionite (S₂O₄²⁻) (59–61). This oxidation state of the Fe protein is paramagnetic, with the four Fe atoms distributed as 3Fe²⁺ and 1Fe³⁺. This state gives rise to an EPR spectrum at low temperatures (~5 K) that has been assigned as a mixture of two spin states (*S* = 1/2 and *S* = 3/2 spin). This mixed spin state has been confirmed in the Mössbauer and MCD spectra. The ratio of the two spin states can be shifted by addition of other reagents such as urea or glycerol into the sample solution (61).

The 1+ oxidation state of the [4Fe–4S] cluster can be reversibly oxidized by the removal of one electron, achieving the 2+ oxidation state (Fe^{Ox}), with the iron atoms distributed as 2Fe²⁺ and 2Fe³⁺ (54, 61, 62). This oxidation state of the [4Fe–4S] cluster is diamagnetic and therefore is EPR silent. The oxidation of the [4Fe–4S] cluster from the 1+ to the 2+ oxidation state can be achieved by the treatment of the Fe protein with redox-active dyes of sufficiently positive potential (e.g., thionine, methylene blue, and indigo disulfonate) (54, 63), whereas reduction from the 2+ to the 1+ oxidation state can be achieved by the addition of a number of reductants (e.g., dithionite) (64). This reversibility allows the establishment of the midpoint reduction potential (*E*_m) for the [4Fe–4S]^{2+/1+} redox couple using

voltametric and coulometric methods (65–67). The values of E_m are dependent on the organism from which the Fe protein is purified and the presence or absence of bound nucleotides (9). The E_m for the $[4\text{Fe-4S}]^{2+/1+}$ couple of the Fe protein from *Azotobacter vinelandii* is measured to be -300 mV in the absence of nucleotides (equation [2]) (62, 68). When MgATP is added to the protein, the E_m value shifts more negative to -430 mV (68). MgADP shifts the E_m to -440 mV (68).

It is well established from kinetic and spectroscopic studies that the $[4\text{Fe-4S}]^{2+/1+}$ redox couple of the $[4\text{Fe-4S}]$ cluster in the Fe protein is functional during the catalytic cycle of nitrogenase (9, 16, 21). While the Fe protein in the $1+$ oxidation state is bound to the MoFe protein, an electron is transferred from the Fe protein to the MoFe protein, resulting in oxidation of the $[4\text{Fe-4S}]$ cluster to the $2+$ oxidation state. The consensus model requires the oxidized Fe protein ($2+$) to dissociate from the MoFe protein and for the $[4\text{Fe-4S}]$ cluster to be reduced back to the $1+$ oxidation state by a reduced electron carrier protein (e.g., flavodoxin or ferredoxin) (51, 52), thereby readying the Fe protein for another round of electron transfer to the MoFe protein.

2.1.2. The Fe Protein Binds Nucleotides

Early work on nitrogenase revealed that the Fe protein could bind nucleotides and that the hydrolysis of nucleotides by the nitrogenase complex was critical to the transfer of an electron from the Fe protein to the MoFe protein (16, 69). The Fe protein binds two nucleotides, one to each subunit. The nucleotide binding sites on the Fe protein are on the opposite end of the Fe protein from the $[4\text{Fe-4S}]$ cluster (30, 31, 37, 38, 41, 43–46). The dissociation constants (K_d) for nucleotide binding to Fe protein have been determined by a number of techniques (70). Recent studies using isothermal titration calorimetry have supported earlier studies showing that the redox state of the $[4\text{Fe-4S}]$ cluster impacts the affinity for nucleotide binding (71). The $2+$ oxidation state binds MgATP with the highest affinity ($K_d = 45$ μM), while the $1+$ oxidation state has a lower affinity ($K_d = 500$ μM) for this nucleotide. Further, these studies have revealed positive cooperativity in the binding of the two nucleotides to both the reduced and oxidized states of the Fe protein (72). For the reduced state (Fe^{Red}) the K_d values for the binding of the first and second MgATP molecules are reported to be $K_{d1} = 500$ μM and $K_{d2} = 170$ μM , respectively. A divalent metal is required for the binding of nucleotides to the Fe protein. While a number of different metals will work, it is thought that Mg^{2+} is the physiologically relevant metal (73). The Fe protein can also bind other nucleotide tri- and di-phosphates (e.g., GTP and GDP) with reasonable affinity, although it is widely believed that ATP and ADP are the relevant nucleotides in vivo (74).

While the Fe protein binds MgATP, it shows undetectable rates of hydrolysis in the absence of the MoFe protein (21). It is only after the Fe protein binds to the MoFe protein that hydrolysis is activated. This observation has been explained from examination of X-ray structures of the Fe protein with bound nucleotides as the movement of a likely catalytic base into place to activate hydrolysis following Fe protein binding to the MoFe protein. A detailed understanding of the specific interactions of nucleotides with the Fe protein has been achieved from the X-ray structures of Fe proteins in various nucleotide-bound states (43–46).

2.1.3. Nucleotide Binding Induces Protein Conformational Changes in the Fe Protein

There is ample evidence showing that the binding of nucleotides to the Fe protein induces conformational changes to the protein structure that impact many aspects of its function. For example, the binding of MgATP or MgADP to the Fe protein shifts the E_m for the $[4\text{Fe-4S}]^{2+/1+}$ redox couple to more negative potentials by about –120 mV (described above). Many other methods also reveal that nucleotides change the properties of the $[4\text{Fe-4S}]$ cluster (16, 21). What is clear is that these changes are not the result of nucleotides binding directly to the $[4\text{Fe-4S}]$ cluster, but rather a result of nucleotide-induced protein conformational changes impacting the cluster over a distance. The nucleotide binding sites are located approximately 15 Å away from the $[4\text{Fe-4S}]$ cluster (30, 31, 37, 38, 41, 43–46). While a number of studies report changes in the electronic properties of the $[4\text{Fe-4S}]$ cluster as a result of nucleotides binding to the Fe protein, it is more recent studies using both small angle X-ray scattering (SAXS) (75) and X-ray crystallography that are providing clearer pictures of the larger structural changes induced in the Fe protein upon nucleotide binding. These are reviewed in other chapters of this volume.

2.2. MoFe Protein

The MoFe protein is an $\alpha_2\beta_2$ heterotetramer ($M_r \sim 250,000$ Da) with the α and β subunits encoded by the *nifD* and *nifK* genes, respectively (9, 49). Each $\alpha\beta$ -dimeric catalytic unit contains one active site metallocluster, the FeMo cofactor ($[7\text{Fe-9S-Mo-X-(R)-homocitrate}]$) (76) and one electron carrier cluster, the P-cluster ($[8\text{Fe-7S}]$). The X-ray crystal structure of the MoFe protein reveals that the FeMo cofactor is embedded solely in the α -subunit, while the P-cluster is located at the interface between the α and β subunits (23, 24). Several structures of the complex of the Fe protein bound to the MoFe protein reveal the interfaces where the Fe protein and MoFe protein dock (43–46). These structures place the P-cluster directly in-line and between the Fe protein $[4\text{Fe-4S}]$ cluster and the FeMo cofactor (**Fig. 2.1**). The distance between the $[4\text{Fe-4S}]$ cluster and the P-cluster varies depending on the nucleotide-bound state of the Fe protein,

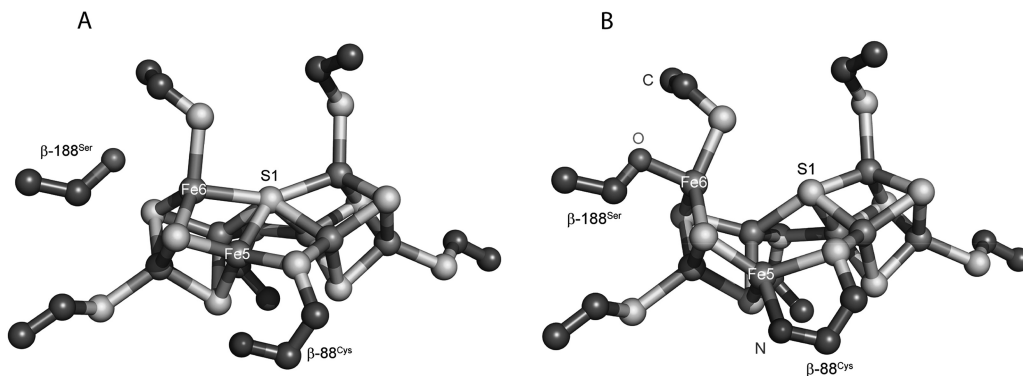


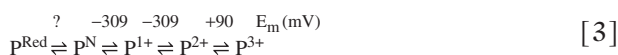
Fig. 2.2. Structure of P-cluster in oxidized and reduced states. The reduced state (P^N) of the P-cluster (**a**) and the oxidized state (P^{Ox}) of the P-cluster (**b**) are shown (3MIN.pdb and 2MIN.pdb, respectively).

leading to a model wherein one role of nucleotides is to alter this electron transfer distance and therefore the electron transfer rate. The arrangement of the three metalloclusters suggests an electron transfer chain from the $[4Fe-4S]$ cluster to the P-cluster and finally to the FeMo-cofactor active site (46).

2.2.1. P-Clusters

Early Mössbauer spectroscopic studies of the MoFe protein revealed that the P-cluster was composed of eight ferrous Fe atoms in the resting state in the presence of dithionite (termed the P^N state) (77). The X-ray structures revealed the nature of this unusual cluster (**Fig. 2.2**) as being composed of two cubic $[4Fe-4S]$ subclusters sharing a common sulfide ligand at one corner (23, 24, 27, 33, 42). Each Fe atom is coordinated by two or three sulfide ligands and one terminal or bridging cysteinyl ligand from a cysteine residue in the α or β subunit. Upon oxidation of the MoFe protein, the P-cluster is oxidized by one or two electrons, which results in significant structural rearrangement (33, 42). Upon oxidation, one of the cubic units is opened up with two Fe-S bonds (Fe5-S1 and Fe6-S1) being cleaved and two novel Fe6-O and Fe5-N bonds being formed. Further, a serinate-O (β -188^{Ser}) and a backbone amide-N (α -88^{Cys}) become ligands to Fe atoms (**Fig. 2.2**) (42).

From in vitro studies using dye oxidants, it has been shown that the resting state of the P-cluster (P^N) can be oxidized by up to three electrons (P^{1+} , P^{2+} , and P^{3+}) (equation [3]) (78–81). The E_m values measured for these redox couples are shown for the *A. vinelandii* MoFe protein as follows (62, 82, 83):



The P^{1+} and P^{2+} oxidation states are often collectively referred to as the P^{Ox} oxidation state, because both oxidation states are

usually populated in oxidized states of the MoFe protein. The P^{3+} oxidation state is not reversible and so is not believed to be functioning during catalysis. More reduced states of the P-cluster from the P^N state have not been observed and seem unlikely given that such a reduction would require reducing Fe atoms beyond the ferrous oxidation state. The E_m for $P^{2+/1+}$ redox couple is pH-dependent, shifting E_m by -53 mV per increase of one pH unit (84). The relevance of this pH dependence is not known, but would be consistent with the coupling of proton and electron transfer reactions involving this cluster.

2.2.2. FeMo Cofactor—The Active Site of Nitrogenase

The FeMo cofactor (76), also called the M-cluster, is embedded in each α subunit of the MoFe protein. The structure of FeMo cofactor was resolved when the X-ray structure of the MoFe protein was solved (47). The structure revealed a heterometallocluster with a composition $[7\text{Fe}-9\text{S}-\text{Mo}-\text{X}-(R)\text{-homocitrate}]$ (**Fig. 2.3**) (28). The cluster is ligated to the peptide matrix through one cysteine ligand (α -275^{Cys}) bound to the Fe atom at one end and through one histidine ligand (α -442^{His}) bound to the Mo atom at the other end. The six Fe atoms in the middle part are arranged as a prismatic structure with each Fe atom coordinated by three sulfide atoms. Recent high-resolution structures of the MoFe protein have revealed the presence of a light atom (C, N, or O) at the center of the Fe cage of unknown identity (designated as X) that is presumed to be bound to each of the central six Fe atoms (28). Homocitrate provides two oxygen atom (C1 carboxylate and C3 hydroxylate) ligands to the Mo (85). Thus, the overall structure of the FeMo cofactor can be viewed as one $[4\text{Fe}-3\text{S}-\text{X}]$

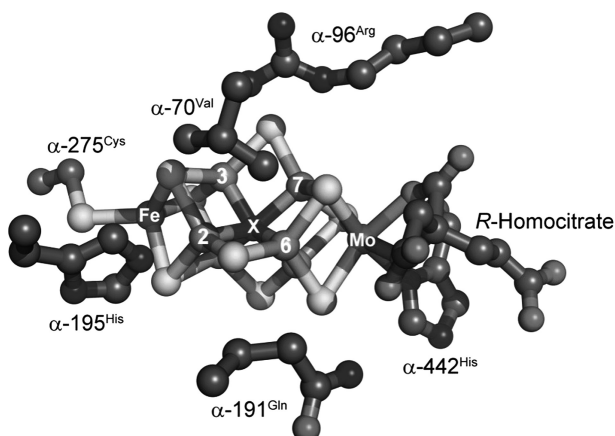


Fig. 2.3. Structure of FeMo cofactor and some of the amino acids surrounding it. Numbering of atoms uses the system in the original structure. Colors for atoms are Fe in *rust*, Mo in *magenta*, S in *yellow*, C in *dark gray*, N in *blue*, and O in *red* (online version only). The figure is generated from PDB file 1M1N.

cubane and one [Mo-3Fe-3S-X] cubane that are connected by three bridging sulfides with one shared μ_6 -X atom at the center.

Identifying the central atom X has proven difficult (69). ENDOR studies have suggested that it is not an exchangeable N atom, but have left open the possibility that it is a non-exchanging N atom (86–88). A vibrational spectroscopy technique (nuclear resonance vibrational spectroscopy or NRVS) supports the presence of a light atom at the center of the Fe cage, but does not resolve the identity of X (89). Likewise, a number of calculations support the presence of X, but do not provide a definitive assignment for X (90–93). To date, there remains no experimental evidence showing the involvement of X in the catalytic cycle of nitrogenase. Obviously, understanding X and its roles in catalysis remains a significant challenge for the field.

FeMo cofactor can be reversibly oxidized or reduced from its resting state. The resting state of FeMo cofactor (M^N) occurs in the MoFe protein isolated in the presence of dithionite. This state is paramagnetic with a rhombic $S = 3/2$ spin EPR signal (94). Treatment of the MoFe protein with oxidizing dyes results in the one-electron oxidation to the M^{Ox} state (77, 78). The M^{Ox} state is diamagnetic ($S = 0$) and EPR silent. The E_m for the M^{Ox}/N redox couple is about -40 mV (95). The M^N state can be reduced. Incubation with the Fe protein in the presence of MgATP and dithionite results in the reduction of FeMo cofactor to an M^R state with an integer spin ($S > 1$) state that is EPR silent (96, 97). The E_m for the M^N/R redox couple has not been measured, but has been estimated as -465 mV (98). The oxidation states of the Fe atoms and the Mo atom in the resting state of FeMo cofactor (M^N) have been examined by Mössbauer and ENDOR spectroscopies. The Mössbauer study suggested an assignment of $[Mo^{4+}, 3Fe^{3+}, 4Fe^{2+}, 9S^{2-}]$ (97), which is supported by calculations using a model with the interstitial X atom (99). The ^{57}Fe ENDOR study suggested an assignment of $[Mo^{4+}, 1Fe^{3+}, 6Fe^{2+}, 9S^{2-}]$ for the resting state FeMo cofactor (100). This later assignment is consistent with the result from calculations on the FeMo cofactor without an interstitial X atom (90). FeMo cofactor must accept multiple electrons (two or more) to complete the reduction of substrates. How these electrons are accumulated on FeMo cofactor is not known. Possible distribution between the P-clusters, FeMo cofactor, and bound intermediates remains to be established.

FeMo cofactor can be extracted from the MoFe protein into organic solvents (76, 101). A number of studies have been conducted on such extracted FeMo cofactor. While some properties of the cofactor in solvent are similar to those for the cofactor in the protein (e.g., EPR spectrum), others are quite different. For example, the reactivity of FeMo cofactor in solvent is different from that of FeMo cofactor bound to the protein (e.g., substrate reduction ability) (102).

A number of studies support FeMo cofactor as the site of substrate (and inhibitor) binding (19, 101), although the precise location of substrate binding is still being pursued (17–19). There are many possibilities for the substrate binding site: (1) the Mo atom; (2) one or more of the central Fe atom(s); and (3) some combination of Fe, S, and Mo atoms. Using spectroscopic methods such as ENDOR, there is growing evidence for binding of hydrides (103), alkynes (104, 105), and nitrogenous compounds (106–110) to one or more of the Fe atoms in the central portion of FeMo cofactor (**Fig. 2.3**). As yet, no experimental results have illustrated binding of any substrate or intermediate to Mo, although this possibility has not been ruled out.

An important tool to gaining insights into substrate binding to FeMo cofactor has been substitution of amino acids in the MoFe protein using site-directed mutagenesis. An early study examined the roles of α -195^{His} in nitrogenase catalysis (**Fig. 2.3**) (111–115). Substitution of the α -195^{His} residue by glutamine resulted in a variant of the MoFe protein that cannot effectively reduce N₂ or azide (N₃[−]), but which retained full rates of reduction of acetylene and protons. From these studies, it was concluded that α -195^{His} might participate in delivery of protons during reduction of nitrogen-containing substrates. Slowing down proton delivery by substituting for α -195^{His} has been exploited to trap presumed intermediate states during the reduction of a

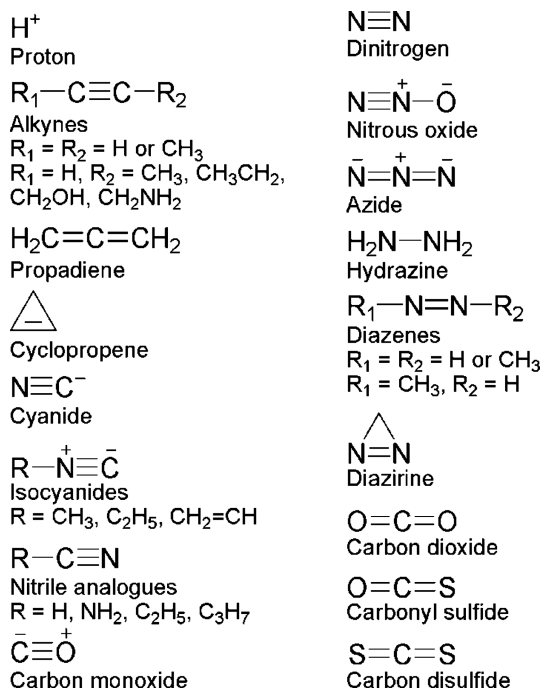


Fig. 2.4. Some substrates for nitrogenase.

number of substrates including hydrazine (N_2H_4) (106, 107), diazene ($\text{HN} = \text{NH}$) (109), and methyldiazene ($\text{MeN} = \text{NH}$) (107, 108). It is clear that $\alpha\text{-195}^{\text{His}}$ is not the sole source of protons for substrate reduction as the rates of reduction of other substrates remain undisturbed when this residue is substituted (115).

Recent work with MoFe proteins containing amino acid substitutions are providing solid evidence for the site of substrate binding on FeMo cofactor. These studies have recently been reviewed (13, 18, 19). While the physiological substrates for nitrogenase are N_2 and protons, a number of other small, multiple bonded compounds have been demonstrated to be substrates. These have been extensively reviewed elsewhere (9, 19, 21, 116). Several of the substrates are shown in **Fig. 2.4**.

3. Nitrogenase Mechanism

3.1. Fe Protein–MoFe Protein Complex Formation

An essential step in the nitrogenase mechanism occurs when the Fe protein, with two bound MgATP molecules, associates with the MoFe protein. This associated complex is fleeting, existing for about 1 s during normal substrate reduction (9). Several events occur while the two proteins are associated, including the hydrolysis of the two MgATP molecules to two MgADP and two P_i molecules and the transfer of one electron from the Fe protein to the MoFe protein. The order of these two events has not been definitively established and is the subject of current studies (19, 20).

The associated state of the nitrogenase complex has been trapped by a number of different approaches. Five different types of stable complexes that have been examined include the following:

- (1) A chemical cross-linked complex using a bifunctional chemical reagent 1-ethyl-3-[3-(dimethylamino)propyl]carbodiimide (EDC) (45, 117, 118).
- (2) A non-dissociating complex formed between the Fe protein from *Clostridium pasteurianum* and the MoFe protein from *A. vinelandii* (119–122).
- (3) A non-dissociating complex formed between an Fe protein with an amino acid deletion ($\Delta 127^{\text{Leu}}$) and the MoFe protein that appears to mimic the ATP-bound state in the absence of ATP (44, 123).
- (4) A non-dissociating complex formed when ADP and AlF_4^- (or BeF_3^-) are added to the Fe protein and MoFe protein. In this case, the AlF_4^- appears to be mimicking the departing phosphate following ATP hydrolysis (43, 124–127).

- (5) Relatively stable complexes of the MoFe protein and the Fe protein with MgADP or β,γ -methylene MgATP bound or without nucleotide bound (46).

Analysis of these tight complexes by a number of different approaches, including X-ray crystallography, is providing insights into the nitrogenase complex such as the following:

- (1) AlF_4^- occupies the binding site where the γ -phosphate portion of MgATP was expected to be (43, 46).
- (2) The subunits of Fe protein are considerably reoriented during complex formation and nucleotide hydrolysis. The movement of two segments of amino acids in the Fe protein (called switches I and II) appears to connect to the [4Fe-4S] cluster, possibly controlling the nucleotide-induced changes in the properties of the [4Fe-4S] cluster (44, 46).
- (3) There are several distinct and mutually exclusive interaction sites on the MoFe protein surface that are selectively populated, depending on the Fe protein nucleotide state (46).
- (4) The distance between the Fe protein [4Fe-4S] cluster and the MoFe protein P-cluster changes by up to 5 Å depending on the nucleotide bound to the Fe protein (46).
- (5) The E_m value of the [4Fe-4S] cluster and the P-cluster is shifted more negative when the two proteins are associated, favoring electron transfer from the Fe protein to the FeMo cofactor (123, 128).

3.2. Fe Protein Cycle

The Fe protein, being an ATP-dependent reductase of the MoFe protein, can be thought of as proceeding through a cycle during its function in the overall nitrogenase catalytic cycle (129, 130). This Fe protein cycle is summarized in **Fig. 2.5**. During nitrogenase catalysis, the reduced Fe protein, with the [4Fe-4S] cluster in its 1+ oxidation state, binds two MgATP molecules. The Fe protein in this state then associates with the MoFe protein (131). Within this complex, MgATP hydrolysis is activated and electron transfer occurs, followed by the dissociation of the two proteins. The spent Fe protein is reactivated by replacing MgADP with MgATP and reducing the 2+ oxidation state to the 1+ oxidation state (**Fig. 2.5**).

While the general features of the Fe protein cycle are known, several important details remain to be resolved. For example, how does complex formation activate MgATP hydrolysis and electron transfer? Which comes first, electron transfer or nucleotide hydrolysis? How specifically is the energy from nucleotide hydrolysis used in the nitrogenase reaction? What specifically is the role of the P-cluster in brokering electrons between the Fe protein

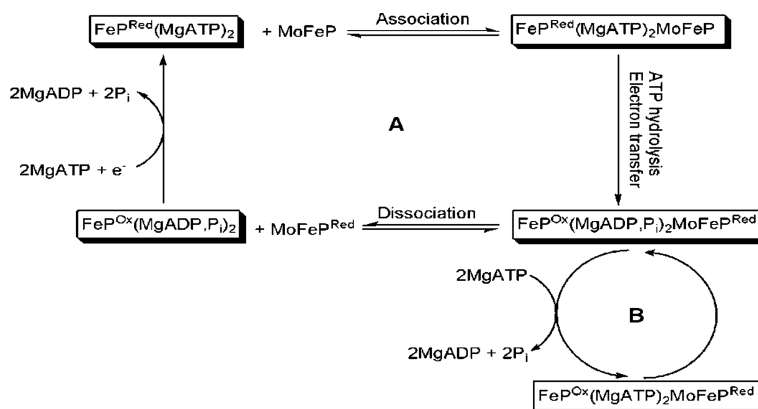


Fig. 2.5. Fe-protein cycle showing the oxidation state changes and MgATP hydrolysis. Abbreviations used are FeP^{Ox} for oxidized Fe protein, FeP^{Red} for reduced Fe protein, MoFeP for the oxidation state of MoFe protein before reduction, and $\text{MoFeP}^{\text{Red}}$ for one more electron reduced state of MoFe protein.

and the active site FeMo cofactor? These and many other questions need to be addressed in the coming years.

3.3. MoFe-Protein Cycle

The MoFe protein must accumulate multiple electrons in order to achieve the reduction of bound substrates. The details of where and how these electrons are accumulated in the MoFe protein are not known (20). A simple notation to designate how many electrons have been transferred into the resting MoFe protein (designated as E_0) is helpful (called the Lowe-Thorneley model) (64, 132–134). This model does not differentiate electrons on the P-cluster from electrons on the FeMo cofactor (Fig. 2.6), but rather simply notes the number of electrons accumulated in the MoFe protein as E_1 , E_2 , etc., with the subscript indicating the number of electrons.

The results of a number of kinetic studies have allowed construction of a MoFe-protein cycle as shown in Fig. 2.6. As

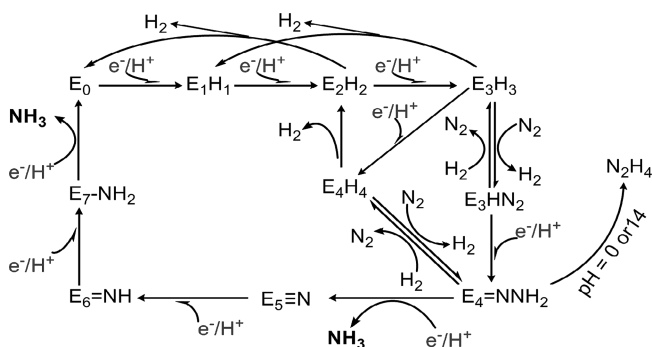


Fig. 2.6. Modified Lowe-Thorneley kinetic scheme for reduction of N_2 . In this scheme, the E_n represents one functional $\alpha\beta$ dimeric unit, which has been reduced by n electrons relative to the resting state E_0 .

noted in the cycle, there is good evidence indicating that different substrates bind to different reduction states (E_n) of the MoFe protein. Dinitrogen is modeled to bind to E_3 or E_4 states (64), which is accompanied by the release of one equivalent of H_2 (22, 135). In the absence of N_2 , the less reduced E_1 and E_2 states are achieved, which are sufficient for proton binding and reduction to H_2 . The non-physiological substrate acetylene is modeled to bind to the E_2 state for reduction to ethylene. The binding of different substrates to different redox states of the MoFe protein can result in confusing inhibition patterns. For example, the inhibition of N_2 reduction by acetylene appears to be non-competitive, while the inhibition of acetylene reduction by N_2 appears to be competitive (136). This apparent contradiction can be explained by the fact that acetylene binds to the E_2 state whereas N_2 binds to more reduced states (64, 137). Thus, acetylene appears to be a non-competitive inhibitor of N_2 reduction and N_2 a competitive inhibitor of acetylene reduction.

Insights into where and to what states of FeMo-cofactor substrates and inhibitors bind have come in recent years from the characterization of freeze-trapped MoFe protein during turnover with substrates or inhibitors. The inhibitor carbon monoxide (CO) has been extensively characterized trapped to FeMo cofactor (100, 138–142). Application of a variety of spectroscopic methods to this trapped state has revealed that at low CO concentrations, a single CO is likely bound bridging between two Fe atoms. At high CO concentrations, two CO molecules are proposed to be bound.

Amino acid substitutions in the MoFe protein have been used, along with freeze trapping to capture a number of different substrates bound as intermediates to FeMo cofactor. The MoFe protein variant, the substrate, and the g values of the EPR spectrum observed are summarized in **Table 2.1**. How these states are trapped is discussed in more detail in another chapter of this volume.

Some of the key findings from characterization of these trapped states include the following:

- (1) A hydride-trapped state is consistent with two hydrides bound to Fe atoms in FeMo cofactor (106).
- (2) The substrate propargyl alcohol and other alkyne substrates have been trapped bound side-on to one or more Fe atoms (104, 105, 143).
- (3) Intermediates have been trapped starting from the nitrogenous substrates hydrazine, diazene, methyldiazene, and N_2 . These intermediates appear to be bound end-on to Fe atom(s) (106–110).
- (4) A specific Fe atom in the central portion of FeMo cofactor has been identified as the likely site of binding of several substrates tested so far (110, 143).

Table 2.1
Important variants of MoFe protein and EPR parameters of the resulting intermediates with different substrates in the turnover state

Mutation	Substrate	EPR parameter	Ref.
Wild type	Dinitrogen (N_2)	$S = 1/2$, $g = 2.08$, 1.99, 1.97	(107, 110)
α -70 ^{Val} →Ala	Propargyl alcohol ($\text{HC}\equiv\text{CCH}_2\text{OH}$)	$S = 1.2$, $g = 2.12$, 2.00, 1.99	(104, 105)
α -70 ^{Val} →Ile	Proton (H^+)	$S = 1/2$, $g = 2.14$, 2.00, 1.96	(103)
α -195 ^{His} →Gln	Methyldiazene ($\text{CH}_3\text{N}=\text{NH}$)	$S = 1.2$, $g = 2.08$, 2.02, 1.99	(107, 108)
α -70 ^{Val} →Ala/ α -195 ^{His} →Gln	Diazene ($\text{HN}=\text{NH}$)	$S = 1/2$, $g = 2.09$, 2.01, 1.93	(109)
α -70 ^{Val} →Ala/ α -195 ^{His} →Gln	Hydrazine ($\text{NH}_2\text{-NH}_2$)	$S = 1/2$, $g = 2.09$, 2.01, 1.93	(106, 107)

These studies have advanced our understanding of where and how substrates interact with the nitrogenase active site. Many other questions remain to be resolved, such as

- (1) Is the N–N bond broken in the trapped nitrogenous species characterized so far?
- (2) What is the level of reduction of the trapped states?
- (3) What is the level of proton addition to the trapped states?
- (4) Do intermediates migrate among the metals (Fe and Mo) during the course of substrate reduction?

Answers to these and many other open questions will greatly advance our understanding of this complex enzyme.

4. Conclusions and Perspectives

Nitrogenase is a complex enzyme that plays a central role in the global N cycle. Great strides have been achieved since its first discovery to understand many facets of this complex system. These advances are largely the result of the application of a wide range of methods, many of which are described in this volume. Clearly, much remains to be resolved about the mechanism of nitrogenase. Future advances will come from the application of the methods summarized in this volume, coupled with application of many new methods. While the prospects for advancing understanding of nitrogenase going forward are good, these advances are not likely to come easily.

Acknowledgments

The authors acknowledge the long collaboration with the Brian Hoffman and Dennis Dean laboratories in advancing understanding of nitrogenase. Work in the laboratory of the authors is supported by a generous grant from the National Institutes of Health (GM59087).

References

- Smil V (2001) Enriching the Earth: Fritz Haber, Carl Bosch, and the Transformation of World Food Production. MIT Press, Cambridge, MA
- Ferguson SJ (1998) Nitrogen cycle enzymology. *Curr Opin Chem Biol* 2:182–193
- Fryzuk MD, MacKay BA (2004) Dinitrogen coordination chemistry: On the biomimetic borderlands. *Chem Rev* 104:385–401
- Haber F (1922) The production of ammonia from nitrogen and hydrogen. *Naturwissenschaften* 10:1041–1049
- Haber F (1923) The history of the ammonia process. *Naturwissenschaften* 11:339–340
- Cheng Q (2008) Perspectives in biological nitrogen fixation research. *J Integr Plant Biol* 50:786–798
- Smith BE (2002) Nitrogen reveals its inner secrets. *Science* 297:1654–1655
- Raymond J, Siefert JL, Staples CR et al (2004) The natural history of nitrogen fixation. *Mol Biol Evol* 21:541–554
- Burgess BK, Lowe DJ (1996) The mechanism of molybdenum nitrogenase. *Chem Rev* 96:2983–3011
- Eady RR (1996) Structure-function relationships of alternative nitrogenases. *Chem Rev* 96:3013–3030
- Bishop PE, Joergers RD (1990) Genetics and molecular biology of alternative nitrogen fixation systems. *Annu Rev Plant Physiol Plant Mol Biol* 41:109–125
- Masepohl B, Schneider K, Drepper T et al (2002) Alternative nitrogenases. In: Leigh GJ (ed) *Nitrogenase Fixation at the Millennium*, pp. 191–222. Elsevier, Amsterdam
- Barney BM, Lee HI, Dos Santos PC et al (2006) Breaking the N₂ triple bond: Insights into the nitrogenase mechanism. *Dalton Trans* 19:2277–2284
- Ribbe M, Gadkari D, Meyer O (1997) N₂ fixation by *Streptomyces thermoautotrophicus* involves a molybdenum- dinitrogenase and a manganese-superoxide oxidoreductase that couple N₂ reduction to the oxidation of superoxide produced from O₂ by a molybdenum-CO dehydrogenase. *J Biol Chem* 272:26627–26633
- Rees DC, Howard JB (2000) Nitrogenase: Standing at the crossroads. *Curr Opin Chem Biol* 4:559–566
- Seefeldt LC, Dean DR (1997) Role of nucleotides in nitrogenase catalysis. *Acc Chem Res* 30:260–266
- Seefeldt LC, Dance I, Dean DR (2004) Substrate interactions with nitrogenase: Fe versus Mo. *Biochemistry* 43:1401–1409
- Dos Santos PC, Igarashi RY, Lee HI et al (2005) Substrate interactions with the nitrogenase active site. *Acc Chem Res* 38:208–214
- Seefeldt LC, Hoffman BM, Dean DR (2009) Mechanism of Mo-dependent nitrogenase. *Annu Rev Biochem* 78:701–722
- Hoffman BM, Dean DR, Seefeldt LC (2009) Climbing nitrogenase: Toward a mechanism of enzymatic nitrogen fixation. *Acc Chem Res* 42:609–619
- Igarashi RY, Seefeldt LC (2003) Nitrogen fixation: The mechanism of the Mo-dependent nitrogenase. *Crit Rev Biochem Mol Biol* 38:351–384
- Simpson FB, Burris RH (1984) A nitrogen pressure of 50 atmospheres does not prevent evolution of hydrogen by nitrogenase. *Science* 224:1095–1097
- Kim J, Rees DC (1992) Crystallographic structure and functional implications of the nitrogenase molybdenum iron protein from *Azotobacter vinelandii*. *Nature* 360:553–560
- Kim J, Rees DC (1992) Structural models for the metal centers in the nitrogenase molybdenum-iron protein. *Science* 257:1677–1682
- Georgiadis MM, Komiya H, Chakrabarti P et al (1992) Crystallographic structure of the nitrogenase iron protein from *Azotobacter vinelandii*. *Science* 257:1653–1659

26. Kim J, Woo D, Rees DC (1993) X-ray crystal structure of the nitrogenase molybdenum-iron protein from *Clostridium pasteurianum* at 3.0-Å resolution. *Biochemistry* 32: 7104–7115
27. Chan MK, Kim J, Rees DC (1993) The nitrogenase FeMo-cofactor and P-cluster pair: 2.2 Å resolution structures. *Science* 260:792–794
28. Einsle O, Tezcan FA, Andrade SLA et al (2002) Nitrogenase MoFe-protein at 1.16 Å resolution: A central ligand in the FeMo-cofactor. *Science* 297:1696–1700
29. Sørle M, Christiansen J, Lemon BJ et al (2001) Mechanistic features and structure of the nitrogenase α -Gln¹⁹⁵ MoFe protein. *Biochemistry* 40:1540–1549
30. Jang SB, Seefeldt LC, Peters JW (2000) Insights into nucleotide signal transduction in nitrogenase: Structure of an iron protein with MgADP bound. *Biochemistry* 39:14745–14752
31. Jang SB, Jeong MS, Seefeldt LC et al (2004) Structural and biochemical implications of single amino acid substitutions in the nucleotide-dependent switch regions of the nitrogenase Fe protein from *Azotobacter vinelandii*. *J Biol Inorg Chem* 9:1028–1033
32. Jang SB, Seefeldt LC, Peters JW (2000) Modulating the midpoint potential of the [4Fe-4S] cluster of the nitrogenase Fe protein. *Biochemistry* 39:641–648
33. Mayer SM, Lawson DM, Gormal CA et al (1999) New insights into structure-function relationships in nitrogenase: A 1.6 Å resolution X-ray crystallographic study of *Klebsiella pneumoniae* MoFe-protein. *J Mol Biol* 292:871–891
34. Mayer SM, Gormal CA, Smith BE et al (2002) Crystallographic analysis of the MoFe protein of nitrogenase from a *nifV* mutant of *Klebsiella pneumoniae* identifies citrate as a ligand to the molybdenum of iron molybdenum cofactor (FeMoco). *J Biol Chem* 277:35263–35266
35. Bolin JT, Ronco AE, Mortenson LE et al (1990) Structure of the nitrogenase MoFe protein: Spatial distribution of the intrinsic metal atoms determined by X-ray anomalous scattering. In: Gresshoff PM, Roth LE, Stacey G, Newton WE (eds) *Nitrogen Fixation: Achievements and Objectives*, pp. 117–124. Chapman and Hall, New York, NY
36. Bolin JT, Campobasso N, Muchmore SW et al (1993) Structure and environment of metal clusters in the nitrogenase molybdenum-iron protein from *Clostridium pasteurianum*. In: Stiefel EI, Coucouvanis D, Newton WE (eds) *Molybdenum Enzymes, Cofactors and Model Systems*, pp. 186–195. ACS, Washington, DC
37. Sen S, Krishnakumar A, McClelland J et al (2006) Insights into the role of nucleotide-dependent conformational change in nitrogenase catalysis: Structural characterization of the nitrogenase Fe protein Leu127 deletion variant with bound MgATP. *J Inorg Biochem* 100:1041–1052
38. Sen S, Igarashi R, Smith A et al (2004) A conformational mimic of the MgATP-bound “on state” of the nitrogenase iron protein. *Biochemistry* 43:1787–1797
39. Schmid B, Ribbe MW, Einsle O et al (2002) Structure of a cofactor-deficient nitrogenase MoFe protein. *Science* 296:352–356
40. Sarma R, Barney BM, Keable S et al (2009) Insights into substrate binding at FeMo-cofactor in nitrogenase from the structure of an α -70^{Leu} MoFe protein variant. *J Inorg Biochem* 104:385–389
41. Jeong MS, Jang SB (2004) Structural basis for the changes in redox potential in the nitrogenase Phe135Trp Fe protein with MgADP bound. *Mol Cells* 18:374–382
42. Peters JW, Stowell MHB, Soltis SM et al (1997) Redox-dependent structural changes in the nitrogenase P-cluster. *Biochemistry* 36:1181–1187
43. Schindelin H, Kisker C, Schlessman JL et al (1997) Structure of ADP-AlF₄[−] stabilized nitrogenase complex and its implications for signal transduction. *Nature* 387:370–376
44. Chiu HJ, Peters JW, Lanzilotta WN et al (2001) MgATP-bound and nucleotide-free structures of a nitrogenase protein complex between the Leu 127^Δ-Fe-protein and the MoFe-protein. *Biochemistry* 40: 641–650
45. Schmid B, Einsle O, Chiu HJ et al (2002) Biochemical and structural characterization of the cross-linked complex of nitrogenase: Comparison to the ADP-AlF₄[−]-stabilized structure. *Biochemistry* 41:15557–15565
46. Tezcan FA, Kaiser JT, Mustafi D et al (2005) Nitrogenase complexes: Multiple docking sites for a nucleotide switch protein. *Science* 309:1377–1380
47. Rees DC, Tezcan FA, Haynes CA et al (2005) Structural basis of biological nitrogen fixation. *Philos Trans R Soc A* 363: 971–984
48. Howard JB, Rees DC (1994) Nitrogenase: A nucleotide-dependent molecular switch. *Annu Rev Biochem* 63:235–264
49. Rubio LM, Ludden PW (2008) Biosynthesis of the Iron-Molybdenum cofactor of nitrogenase. *Annu Rev Microbiol* 62:93–111

50. Hu Y, Fay AW, Lee CC et al (2008) Assembly of nitrogenase MoFe protein. *Biochemistry* 47:3973–3981
51. Martin AE, Burgess BK, Iismaa SE et al (1989) Construction and characterization of an *Azotobacter vinelandii* strain with mutations in the genes encoding flavodoxin and ferredoxin I. *J Bacteriol* 171:3162–3167
52. Mortenson LE (1964) Ferredoxin requirement for nitrogen fixation by extracts of *Clostridium pasteurianum*. *Biochim Biophys Acta* 81:473–478
53. Angove HC, Yoo SJ, Burgess BK et al (1997) Mössbauer and EPR evidence for an all-ferrous Fe₄S₄ cluster with *S* = 4 in the Fe protein of nitrogenase. *J Am Chem Soc* 119:8730–8731
54. Watt GD, Reddy KRN (1994) Formation of an all ferrous Fe₄S₄ cluster in the iron protein component of *Azotobacter vinelandii* nitrogenase. *J Inorg Biochem* 53:281–294
55. Musgrave KB, Angove HC, Burgess BK et al (1998) All-ferrous titanium(III) citrate reduced Fe protein of nitrogenase: An XAS study of electronic and metrical structure. *J Am Chem Soc* 120:5325–5326
56. Strop P, Takahara PM, Chiu HJ et al (2001) Crystal structure of the all-ferrous [4Fe-4S]⁰ form of the nitrogenase iron protein from *Azotobacter vinelandii*. *Biochemistry* 40:651–656
57. Yoo SJ, Angove HC, Burgess BK et al (1998) Magnetic circular dichroism study of the all-ferrous [4Fe-4S] cluster of the Fe-protein of *Azotobacter vinelandii* nitrogenase. *J Am Chem Soc* 120:9704–9705
58. Nyborg AC, Johnson JL, Gunn A et al (2000) Evidence for a two-electron transfer using the all-ferrous Fe protein during nitrogenase catalysis. *J Biol Chem* 275:39307–39312
59. Hagen WR, Dunham WR, Braaksma A et al (1985) On the prosthetic group(s) of component II from nitrogenase: EPR of the Fe-protein from *Azotobacter vinelandii*. *FEBS Lett* 187:146–150
60. Hagen WR, Eady RR, Dunham WR et al (1985) A novel *S* = 3/2 EPR signal associated with native Fe proteins of nitrogenase. *FEBS Lett* 189:250–254
61. Lindahl PA, Day EP, Kent TA et al (1985) Mössbauer, EPR, and magnetization studies of the *Azotobacter vinelandii* Fe protein. *J Biol Chem* 260:11160–11173
62. Thorneley RNF, Ashby GA (1989) Oxidation of nitrogenase iron protein by dioxygen without inactivation could contribute to high respiration rates of *Azotobacter* species and facilitate nitrogen fixation in other aerobic environments. *Biochem J* 261:181–187
63. Larsen C, Christensen S, Watt GD (1995) Reductant-independent ATP hydrolysis catalyzed by homologous nitrogenase proteins from *Azotobacter vinelandii* and heterologous crosses with *Clostridium pasteurianum*. *Arch Biochem Biophys* 323:215–222
64. Thorneley RNF, Lowe DJ (1985) Kinetics and mechanisms of the nitrogenase enzyme system. In: Spiro TG (ed) *Molybdenum Enzymes*, pp. 221–284. Wiley, New York, NY
65. Ryle MJ, Lanzilotta WN, Mortenson LE et al (1995) Evidence for a central role of lysine 15 of *Azotobacter vinelandii* nitrogenase iron protein in nucleotide binding and protein conformational changes. *J Biol Chem* 270:13112–13117
66. Watt GD (1979) An electrochemical method for measuring redox potentials of low potential proteins by microcoulometry at controlled potentials. *Anal Biochem* 99:399–407
67. Watt GD, Wang ZC, Knotts RR (1986) Redox reactions of and nucleotide binding to the iron protein of *Azotobacter vinelandii*. *Biochemistry* 25:8156–8162
68. Lanzilotta WN, Ryle MJ, Seefeldt LC (1995) Nucleotide hydrolysis and protein conformational changes in *Azotobacter vinelandii* nitrogenase iron protein: Defining the function of aspartate 129. *Biochemistry* 34:10713–10723
69. Peters JW, Szilagyi RK (2006) Exploring new frontiers of nitrogenase structure and mechanism. *Curr Opin Chem Biol* 10:101–108
70. Yates MG (1991) The enzymology of molybdenum-dependent nitrogen fixation. In: Stacey G, Burris RH, Evans HJ (eds) *Biological Nitrogen Fixation*, pp. 685–735. Chapman and Hall, New York, NY
71. Lanzilotta WN, Parker VD, Seefeldt LC (1999) Thermodynamics of nucleotide interactions with the *Azotobacter vinelandii* nitrogenase iron protein. *Biochim Biophys Acta* 1429:411–421
72. Cordewener J, Haaker H, Van Ewijk P et al (1985) Properties of the MgATP and MgADP binding sites on the Fe protein of nitrogenase from *Azotobacter vinelandii*. *Eur J Biochem* 148:499–508
73. Weston MF, Kotake S, Davis LC (1983) Interaction of nitrogenase with nucleotide analogs of ATP and ADP and the effect of metal ions on ADP inhibition. *Arch Biochem Biophys* 225:809–817
74. Ryle MJ, Seefeldt LC (2000) Hydrolysis of nucleoside triphosphates other than

- ATP by nitrogenase. *J Biol Chem* 275: 6214–6219
75. Sarma R, Mulder DW, Brecht E et al (2007) Probing the MgATP-bound conformation of the nitrogenase Fe protein by solution small-angle X-ray scattering. *Biochemistry* 46:14058–14066
76. Shah VK, Brill WJ (1977) Isolation of an iron-molybdenum cofactor from nitrogenase. *Proc Natl Acad Sci USA* 74:3249–3253
77. Zimmermann R, Münck E, Brill WJ et al (1978) Nitrogenase X: Mössbauer and EPR studies on reversibly oxidized MoFe protein from *Azotobacter vinelandii* OP: Nature of the iron centers. *Biochim Biophys Acta* 537:185–207
78. Lindahl PA, Papaefthymiou V, Orme-Johnson WH et al (1988) Mössbauer studies of solid thionin-oxidized MoFe protein of nitrogenase. *J Biol Chem* 263: 19412–19418
79. Hagen WR, Wassink H, Eady RR et al (1987) Quantitative EPR of an $S = 7/2$ system in thionine-oxidized MoFe proteins of nitrogenase: A redefinition of the P-cluster concept. *Eur J Biochem* 169:457–465
80. Pierik AJ, Wassink H, Haaker H et al (1993) Redox properties and EPR spectroscopy of the P-clusters of *Azotobacter vinelandii* MoFe protein. *Eur J Biochem* 212:51–61
81. Tittsworth RC, Hales BJ (1993) Detection of EPR signals assigned to the 1-equiv-oxidized P-clusters of the nitrogenase MoFe protein from *Azotobacter vinelandii*. *J Am Chem Soc* 115:9763–9767
82. Lanzilotta WN, Fisher K, Seefeldt LC (1997) Evidence for electron transfer-dependent formation of a nitrogenase iron protein-molybdenum-iron protein tight complex: The role of aspartate 39. *J Biol Chem* 272:4157–4165
83. Morgan TV, Mortenson LE, McDonald JW et al (1988) Comparison of redox and EPR properties of the molybdenum iron proteins of *Clostridium pasteurianum* and *Azotobacter vinelandii* nitrogenases. *J Inorg Biochem* 33:111–120
84. Lanzilotta WN, Christiansen J, Dean DR et al (1998) Evidence for coupled electron and proton transfer in the [8Fe-7S] cluster of nitrogenase. *Biochemistry* 37: 11376–11384
85. Hoover TR, Robertson AD, Cerny RL et al (1987) Identification of the V factor needed for the synthesis of the iron-molybdenum cofactor of nitrogenase as homocitrate. *Nature* 329:855–857
86. Lee HI, Benton PM, Laryukhin M et al (2003) The interstitial atom of the nitrogenase FeMo-cofactor: ENDOR and ESEEM show it is not an exchangeable nitrogen. *J Am Chem Soc* 125:5604–5605
87. Yang TC, Maeser NK, Laryukhin M et al (2005) The interstitial atom of the nitrogenase FeMo-cofactor: ENDOR and ESEEM evidence that it is not a nitrogen. *J Am Chem Soc* 127:12804–12805
88. Lukoyanov D, Pelmenschikov V, Maeser N et al (2007) Testing if the interstitial atom, X, of the nitrogenase molybdenum-iron cofactor is N or C: ENDOR, ESEEM, and DFT studies of the $S = 3/2$ resting state in multiple environments. *Inorg Chem* 46: 11437–11449
89. George SJ, Igarashi RY, Xiao Y et al (2008) Extended X-ray absorption fine structure and nuclear resonance vibrational spectroscopy reveal that NifB-co, a FeMo-co precursor, comprises a 6Fe core with an interstitial light atom. *J Am Chem Soc* 130: 5673–5680
90. Lovell T, Li J, Liu T et al (2001) FeMo cofactor of nitrogenase: A density functional study of states M^N , M^{OX} , M^R , and M^I . *J Am Chem Soc* 123:12392–12410
91. Pelmenschikov V, Case DA, Noodleman L (2008) Ligand-bound $S = 1/2$ FeMo-cofactor of nitrogenase: Hyperfine interaction analysis and implication for the central ligand X identity. *Inorg Chem* 47: 6162–6172
92. Dance I (2003) The consequences of an interstitial N atom in the FeMo cofactor of nitrogenase. *Chem Commun* 3: 324–325
93. Dance I (2007) The mechanistically significant coordination chemistry of dinitrogen at FeMo-co, the catalytic site of nitrogenase. *J Am Chem Soc* 129:1076–1088
94. Orme-Johnson WH, Hamilton WD, Jones TL et al (1972) Electron paramagnetic resonance of nitrogenase and nitrogenase components from *Clostridium pasteurianum* W5 and *Azotobacter vinelandii* OP. *Proc Natl Acad Sci USA* 69:3142–3145
95. Schultz FA, Gheller SF, Newton WE (1988) Iron molybdenum cofactor of nitrogenase: Electrochemical determination of the electron stoichiometry of the oxidized/semi-reduced couple. *Biochem Biophys Res Commun* 152:629–635
96. Huynh BH, Henzl MT, Christner JA et al (1980) Nitrogenase XII: Mössbauer studies of the MoFe protein from *Clostridium pasteurianum* W5. *Biochim Biophys Acta* 623:124–138
97. Yoo SJ, Angove HC, Papaefthymiou V et al (2000) Mössbauer study of the MoFe protein

- of nitrogenase from *Azotobacter vinelandii* using selective ^{57}Fe enrichment of the M-centers. *J Am Chem Soc* 122:4926–4936
98. Watt GD, Burns A, Lough S et al (1980) Redox and spectroscopic properties of oxidized MoFe protein from *Azotobacter vinelandii*. *Biochemistry* 19:4926–4932
99. Lovell T, Liu T, Case DA et al (2003) Structural, spectroscopic, and redox consequences of a central ligand in the FeMoco of nitrogenase: A density functional theoretical study. *J Am Chem Soc* 125:8377–8383
100. Lee HI, Hales BJ, Hoffman BM (1997) Metal-ion valencies of the FeMo cofactor in CO-inhibited and resting state nitrogenase by ^{57}Fe Q-band ENDOR. *J Am Chem Soc* 119:11395–11400
101. Burgess BK (1990) The iron-molybdenum cofactor of nitrogenase. *Chem Rev* 90:1377–1406
102. Smith BE, Durrant MC, Fairhurst SA et al (1999) Exploring the reactivity of the isolated iron-molybdenum cofactor of nitrogenase. *Coord Chem Rev* 185:669–687
103. Igarashi RY, Laryukhin M, Dos Santos PC et al (2005) Trapping H^- bound to the nitrogenase FeMo-cofactor active site during H_2 evolution: Characterization by ENDOR spectroscopy. *J Am Chem Soc* 127:6231–6241
104. Benton PMC, Laryukhin M, Mayer SM et al (2003) Localization of a substrate binding site on FeMo-cofactor in nitrogenase: Trapping propargyl alcohol with an α -70-substituted MoFe protein. *Biochemistry* 42:9102–9109
105. Lee HI, Igarashi RY, Laryukhin M et al (2004) An organometallic intermediate during alkyne reduction by nitrogenase. *J Am Chem Soc* 126:9563–9569
106. Barney BM, Laryukhin M, Igarashi RY et al (2005) Trapping a hydrazine reduction intermediate on the nitrogenase active site. *Biochemistry* 44:8030–8037
107. Barney BM, Yang TC, Igarashi RY et al (2005) Intermediates trapped during nitrogenase reduction of N_2 , $\text{CH}_3\text{-N=NH}$, and $\text{H}_2\text{N-NH}_2$. *J Am Chem Soc* 127:14960–14961
108. Barney BM, Lukoyanov D, Yang TC et al (2006) A methyldiazene (HN=N-CH_3) derived species bound to the nitrogenase active site FeMo-cofactor: Implications for mechanism. *Proc Natl Acad Sci USA* 103:17113–17118
109. Barney BM, McClead J, Lukoyanov D et al (2007) Diazene (HN=NH) is a substrate for nitrogenase: Insights into the pathway of N_2 reduction. *Biochemistry* 46:6784–6794
110. Barney BM, Lukoyanov D, Igarashi RY et al (2009) Trapping an intermediate of dinitrogen (N_2) reduction on nitrogenase. *Biochemistry* 48:9094–9102
111. Kim CH, Newton WE, Dean DR (1995) Role of the MoFe protein α -subunit histidine-195 residue in FeMo-cofactor binding and nitrogenase catalysis. *Biochemistry* 34:2798–2808
112. Thomann H, Bernardo M, Newton WE et al (1991) N coordination of MoFe cofactor requires His-195 of the MoFe protein α -subunit and is essential for biological nitrogen fixation. *Proc Natl Acad Sci USA* 88:6620–6623
113. Scott DJ, May HD, Newton WE et al (1990) Role for the nitrogenase MoFe protein α -subunit in FeMo-cofactor binding and catalysis. *Nature* 343:188–190
114. Dilworth MJ, Fisher K, Kim CH et al (1998) Effects on substrate reduction of substitution of histidine-195 by glutamine in the α -subunit of the MoFe protein of *Azotobacter vinelandii* nitrogenase. *Biochemistry* 37:17495–17505
115. Fisher K, Dilworth MJ, Newton WE (2000) Differential effects on N_2 binding and reduction, HD formation, and azide reduction with α -195^{His}- and α -191^{Gln}-substituted MoFe proteins of *Azotobacter vinelandii* nitrogenase. *Biochemistry* 39:15570–15577
116. Burgess BK (1985) Substrate reactions of nitrogenase. In: Spiro TG (ed) *Metal Ions in Biology: Molybdenum Enzymes*, pp. 161–219. Wiley, New York, NY
117. Willing AH, Georgiadis MM, Rees DC et al (1989) Cross-linking of nitrogenase components. *J Biol Chem* 264:8499–8503
118. Willing A, Howard JB (1990) Crosslinking site in *Azotobacter vinelandii* complex. *J Biol Chem* 265:6596–6599
119. Emerich DW, Burris RH (1976) Interactions of heterologous nitrogenase components that generate catalytically inactive complexes. *Proc Natl Acad Sci USA* 73:4369–4373
120. Emerich DW, Burris RH (1978) Complementary functioning of the component proteins of nitrogenase from several bacteria. *J Bacteriol* 134:936–943
121. Emerich DW, Ljones T, Burris RH (1978) Nitrogenase: Properties of the catalytically inactive complex between the *Azotobacter vinelandii* MoFe protein and the *Clostridium pasteurianum* Fe protein. *Biochim Biophys Acta* 527:359–369
122. Chan JM, Ryle MJ, Seefeldt LC (1999) Evidence that MgATP accelerates primary

- electron transfer in a *Clostridium pasteurianum* Fe protein-*Azotobacter vinelandii* MoFe protein nitrogenase tight complex. J Biol Chem 274:17593–17598
123. Lanzilotta WN, Seefeldt LC (1997) Changes in the midpoint potentials of the nitrogenase metal centers as a result of iron protein-molybdenum-iron protein complex formation. Biochemistry 36: 12976–12983
 124. Clarke TA, Yousafzai FK, Eady RR (1999) *Klebsiella pneumoniae* nitrogenase: Formation and stability of putative beryllium fluoride-ADP transition state complexes. Biochemistry 38:9906–9913
 125. Duyvis MG, Wassink H, Haaker H (1996) Formation and characterization of a transition state complex of *Azotobacter vinelandii* nitrogenase. FEBS Lett 380: 233–236
 126. Renner KA, Howard JB (1996) Aluminum fluoride inhibition of nitrogenase: Stabilization of a nucleotide-Fe-protein-MoFe protein complex. Biochemistry 35: 5353–5358
 127. Miller RW, Eady RR, Fairhurst SA et al (2001) Transition state complexes of the *Klebsiella pneumoniae* nitrogenase proteins: Spectroscopic properties of aluminum fluoride-stabilized and beryllium fluoride-stabilized MgADP complexes reveal conformational differences of the Fe protein. Eur J Biochem 268:809–818
 128. Spee JH, Arendsen AF, Wassink H et al (1998) Redox properties and electron paramagnetic resonance spectroscopy of the transition state complex of *Azotobacter vinelandii* nitrogenase. FEBS Lett 432: 55–58
 129. Duyvis MG, Wassink H, Haaker H (1998) Nitrogenase of *Azotobacter vinelandii*: Kinetic analysis of the Fe protein redox cycle. Biochemistry 37:17345–17354
 130. Christiansen J, Dean DR, Seefeldt LC (2001) Mechanistic features of the Mo-containing nitrogenase. Annu Rev Plant Physiol Plant Mol Biol 52:269–295
 131. Hageman RV, Burris RH (1978) Nitrogenase and nitrogenase reductase associate and dissociate with each catalytic cycle. Proc Natl Acad Sci USA 75:2699–2702
 132. Lowe DJ, Thorneley RNF (1984) The mechanism of *Klebsiella pneumoniae* nitrogenase action: The determination of rate constants required for the simulation of kinetics of N₂ reduction and H₂ evolution. Biochem J 224:895–901
 133. Thorneley RNF, Lowe DJ (1984) The mechanism of *Klebsiella pneumoniae* nitrogenase action: Pre-steady-state kinetics of an enzyme-bound intermediate in N₂ reduction and of NH₃ formation. Biochem J 224: 887–894
 134. Thorneley RNF, Lowe DJ (1984) The mechanism of *Klebsiella pneumoniae* nitrogenase action: Stimulation of the dependences of H₂-evolution rate on component-protein concentration and ratio and sodium dithionite concentration. Biochem J 224:903–909
 135. Liang J, Burris RH (1988) Hydrogen burst associated with nitrogenase-catalyzed reactions. Proc Natl Acad Sci USA 85: 9446–9450
 136. Rivera-Ortiz JM, Burris RH (1975) Interactions among substrates and inhibitors of nitrogenase. J Bacteriol 123:537–545
 137. Davis LC, Shah VK, Brill WJ (1975) Nitrogenase: Effect of component ratio, ATP and H₂ on the distribution of electrons to alternative substrates. Biochim Biophys Acta 403:67–78
 138. Lee HI, Cameron LM, Hales BJ et al (1997) CO binding to the FeMo cofactor of CO-inhibited nitrogenase: ¹³C and ¹H Q-band ENDOR investigation. J Am Chem Soc 119:10121–10126
 139. Pollock CR, Lee HI, Cameron LM et al (1995) Investigation of CO bound to inhibited forms of nitrogenase MoFe protein by ¹³C ENDOR. J Am Chem Soc 117: 8686–8687
 140. Christie PD, Lee HI, Cameron LM et al (1996) Identification of the CO-binding cluster in nitrogenase MoFe protein by ENDOR of ⁵⁷Fe isotopomers. J Am Chem Soc 118:8707–8709
 141. Maskos Z, Hales BJ (2003) Photo-lability of CO bound to Mo-nitrogenase from *Azotobacter vinelandii*. J Inorg Biochem 93:11–17
 142. Maskos Z, Fisher K, Sørleie M et al (2005) Variant MoFe proteins of *Azotobacter vinelandii*: Effects of carbon monoxide on electron paramagnetic resonance spectra generated during enzyme turnover. J Biol Inorg Chem 10:394–406
 143. Dos Santos PC, Mayer SM, Barney BM et al (2007) Alkyne substrate interaction within the nitrogenase MoFe protein. J Inorg Biochem 101:1642–1648

Nitrogen Fixation

Methods and Protocols

Ribbe, M.W. (Ed.)

2011, X, 326 p. 72 illus., Hardcover

ISBN: 978-1-61779-193-2

A product of Humana Press